Adsorption of Multiple H_2 Molecules on Pd_3 and Pd_4 Clusters. A Density Functional Study

Jerzy Moc,[†] **Djamaladdin G. Musaev,*** **and Keiji Morokuma***

Cherry L. Emerson Center for Scientific Computation and Department of Chemistry, Emory University, Atlanta, Georgia 30322

Received: June 20, 2000; In Final Form: October 2, 2000

The reaction/adsorption of multiple H_2 molecules on Pd_n clusters with $n = 3$ and 4 were studied using the density functional theory. It has been shown that the activation of the first H_2 molecule by Pd_3 and Pd_4 takes place without or with a small energetic barrier (based on ΔH (298.15 K)) and leads to the formation of $Pd_3(H)_2$ and $Pd_4(H)_2$ complexes, respectively, where the H−H bond is broken. For the $Pd_4(H)_2$ complex, various isomeric structures were found in the singlet and triplet states, among which the singlet **Pd4_1_c_(e,e′)**, with the two H ligands bridging the Pd−Pd edges not sharing the Pd atom, is found to be the most favorable. Unlike the first H_2 addition reaction, dissociative adsorption of the second H_2 molecule, reactions $Pd_3(H)_2 + H_2 \rightarrow Pd_3(H)_4$ and $Pd_4(H)_2 + H_2 \rightarrow Pd_4(H)_4$, appeared to be thermodynamically and kinetically unfavorable. Instead, molecular adsorption of additional mH_2 molecules onto the "naked" Pd centers of the $Pd_3(H)_2$ and $Pd_4(H)_2$ complexes was shown to be feasible, which is in good agreement with the experimental $Pd_n + D_2$ saturation studies. The thermodynamic stabilities of the resulting $Pd_3(H)_2(H_2)_m$ ($m = 1-3$) and $Pd_4(H)_2(H_2)_m$ ($m = 1-4$) species were discussed in terms of the ΔH and ΔG values estimated at $T = 298.15$ and 70 K.

I. Introduction

Atomic and molecular clusters have been extensively investigated for the last couple of decades, both experimentally and theoretically.[1] Those clusters consisting of transition metal (TM) atoms such as Pd or Pt are of particular interest because of their technological importance in heterogeneous catalysis. It has been inferred from gas-phase reactivity studies that small TM clusters exhibit properties that differ fundamentally from the corresponding bulk metal.[2] Strong size-dependence of reactivity of metal clusters has been observed in many cases,[3,4] especially with molecular hydrogen.[2,3a,3b,3f−3i,4]

From a computational point of view, TM clusters provide an excellent opportunity to address various structural, electronic, and reactivity issues. In recent papers,[5,6] we have studied activation of the *first* H_2 and CH_4 molecules on Pt_n and Pd_n clusters with $n = 2, 3$, using the density functional theory (DFT) method with the B3LYP functional and CASPT2 (complete active space second-order perturbation) methods. For the Pt and Pd atoms and Pt_2 and Pd_2 dimers, B3LYP proved to yield reliable electronic structures as verified against the CASPT2 calculations and experimental data.[5] For chemical reactions of metal clusters, full geometry optimization was found to be essential to model such processes.[5,6] Activation of the H_2 reactant by the Pt_2 dimer and the Pt_3 trimer was shown to occur on the single metal atom, followed by H migration to the other Pt atom(s) with a negligible barrier. The above mechanism differed from that operative for Pd_2 and Pd_3, where the metal atoms work "collaboratively" to break the H−H bond without (or with a very small) barrier.[5,6] Consequently, we have found different mechanisms of the H−H (and C−H) bond activation on Pt_n and Pd_n clusters studied; this reaction occurred on the top of the former, but on the edge of the latter, clusters.

In the present work, we extend the theoretical DFT study of reactivity of palladium clusters toward H_2 by considering both the Pd_4 tetramer and the interaction of Pd_3 and Pd_4 with multiple H_2 molecules. Our results are relevant to the experimental observations by Cox et al.[4] on the chemisorption of simple molecules, including H_2 and D_2, on small unsupported Pd_n clusters ($n < 25$). In particular, on the basis of the saturation studies with D_2, these authors concluded that the resulting clusters were "hydrogen rich", i.e., that they had a D/Pd ratio greater than 1. The latter ratio was also shown to approach unity as the cluster size increased.[4]

Three issues we wish to address here are as follows: (1) How many H_2 molecules can Pd_3 and Pd_4 clusters accommodate? (2) What are the reaction mechanisms for adsorption of the consecutive H_2 molecules on these clusters? (3) What are the actual structures and spin states of the corresponding products?

II. Computational Methods

Optimized structures and normal-mode frequencies were calculated using the B3LYP method[7,8] and the relativistic effective core potential (ECP) of Wadt and Hay with the valence double-ζ (VDZ) basis set[9] on Pd in conjunction with the DZ basis[10] for H (BSI, below). The energetics were improved using the relativistic ECP of Dolg et al. on Pd and the associated valence triple-ζ (VTZ) basis[11] combined with Dunning's[12] augmented correlation-consistent basis for H (BSII, below).[13] Spin-restricted and spin-unrestricted calculations were carried out for singlets and triplets, respectively. For activation reaction paths, minima were connected to each transition state (TS) by following the intrinsic reaction coordinate (IRC).[14] Enthalpies and Gibbs free energies were calculated at both room temperature ($T = 298.15$ K) and low temperature (70 K)[15] at 1 atm, using vibrational frequencies evaluated at the B3LYP/BSI level. (Note that the actual cluster temperature in the experiment by

---

* To whom correspondence should be addressed.

[†] Permanent address: Faculty of Chemistry, Wroclaw University, F. Joliot-Curie 14, 50-383 Wroclaw, Poland.

10.1021/jp0022104 CCC: \$19.00

TABLE 1: Energies and Thermodynamic Values (kcal/mol) for Reactions Involving Pd_3 Clusters Calculated at the B3LYP/BSII Level

	ΔE		$T = 298.15$ K		$T = 70$ K	
reaction species[a]		ΔZPE	ΔH	ΔG	ΔH	ΔG
$Pd_3(^3B_2) + H_2$	0.0	0.0	0.0	0.0	0.0	0.0
$Pd_3(^1A_1) + H_2$	4.8	4.9	4.9	5.8	4.9	5.1
$Pd_3(H_2)$(**Pd3_1_a**)	−8.2	−5.7	−6.9	1.2	−6.2	−4.6
$Pd_3(H_2)$ ($^3A'$)(**Pd3_1_a**)	−10.9	−8.9	−9.8	−3.1	−9.3	−8.0
1st H_2 act TS (**Pd3_1_b**)	−1.7	−1.5	−3.0	5.5	−2.0	−0.5
1st H_2 act TS (^3A) (**Pd3_1_b**)	−1.8	−1.6	−2.6	3.7	−2.0	−0.8
$Pd_3(H)_2$ (**Pd3_1_c_(e,f)**)	−34.5	−33.3	−34.8	−26.4	−33.8	−32.3
$Pd_3(H)_2$ ($^3A''$)(**Pd3_1_c_(t,e)**)	−16.4	−16.0	−17.0	−10.0	−16.4	−15.1
$Pd_3(H)_2$ (**Pd3_1_c_(e,f)**) [+ mH2]	0.0	0.0	0.0	0.0	0.0	0.0
$Pd_3(H)_2(H_2)$(**Pd3_2_a_(e,f)**)	−13.1	−11.0	−11.7	−5.6	−11.3	−10.1
$Pd_3(H)_2(H_2)$(**Pd3_2_a_(e,e)**)	−10.9	−7.7	−8.6	−1.7	−8.1	−6.8
$Pd_3(H)_2(H_2)$(**Pd3_2_a′_(e,f)**)	−11.3	−9.1	−10.0	−3.1	−9.6	−8.2
2nd H_2 act TS (**Pd3_2_b**)	8.5	9.7	7.9	17.0	9.3	10.7
*2nd H_2 act TS (**Pd3_2_b**) reverse*[b]	*0.0*	*−0.2*	*−0.6*	*0.5*	*−0.2*	*−0.2*
$Pd_3(H)_4$(**Pd3_2_c_(t,e,e,e)**)	8.5	9.9	8.5	16.5	9.5	10.9
$Pd_3(H)_2(H_2)_2$(**Pd3_3_a_(e,f)**)	−23.5	−19.1	−20.8	−7.2	−19.9	−17.2
$Pd_3(H)_2(H2)_3$(**Pd3_4_a_(e,f)**)	−35.0	−28.0	−30.7	−10.1	−29.3	−25.2

[a] If not indicated, the electronic state of the system is a closed-shell singlet. [b] Relative to the $Pd_3(H)_4$(**Pd3_2_c_(t,e,e,e)**) product.

Cox et al.[4] was not reported.) The calculations were performed using Gaussian 98.[16]

To present our results in a systematic way, we have introduced the **Pd*n*_x_y_z** notation for the calculated structures. Here "***n***" indicates the number of TM atoms in the cluster (in this paper $n = 3$ and 4); "**x**" shows which H_2 molecule (**1**st, **2**nd, **3**rd, etc.) participates in the reaction; "**y**" describes the nature of the species: **y** = **a** (or **a′**) indicates the initial dihydrogen complex, **y** = **b** corresponds to the H−H activation TS, **y** = **c** indicates the H−H activated product, and **y** = **d** (**d1**, etc.) is assigned to the isomerization TS; and "**z**" shows the position of the H-ligands in the activated system. In the activated system, the H-ligand can be positioned (1) on the single (terminal) Pd atom (we call this site "**t**"), (2) on the edge of the Pd−Pd bond (this site is denoted "**e**"), or (3) on the plane of the Pd−Pd−Pd face (this site is termed "**f**"). Because the systems calculated here have an even number of H-ligands, "**z**" will have an even number of components, and (**e,e**) indicates that the two H-ligands bridge the Pd−Pd edges sharing the Pd atom; (**e,e′**) shows that the two H-ligands bridge the Pd−Pd edges not sharing the Pd atom; (**e,f**) shows that the first H-ligand bridges the Pd−Pd edge and the second H-ligand caps the Pd−Pd−Pd face, which shares the Pd−Pd edge; (**e,f ′**) indicates that the first H-ligand bridges the Pd−Pd edge and the second H-ligand caps the Pd−Pd−Pd face, which does not share the Pd−Pd edge, and so on.

III. Results and Discussion

In Tables 1 and 2 we summarize relative energies and thermodynamic values for reactions involving Pd_3 and Pd_4 clusters, respectively. Structures relevant to Pd_3 are drawn in Figures 1 and 2, and ΔH and ΔG of the reactions/adsorptions $Pd_3(H)_2 + mH_2 \rightarrow Pd_3(H)_2(H_2)_m$ ($m = 1-3$) compared in Figure 3. For Pd_4, structures are depicted in Figures 4, 6, and 7, the first H_2 activation ΔH profile is given in Figure 5, and ΔH and ΔG of the reactions/adsorptions $Pd_4(H)_2 + mH_2 \rightarrow Pd_4(H)_2(H_2)_m$ ($m = 1-4$) are presented in Figure 8. Below we discuss only B3LYP/BSII thermodynamic results. The lower-level B3LYP/BSI values are listed in Tables S1 and S2 (Supporting Information) for comparison purposes.

A. Reaction of the H_2 molecule with Pd_3. Our previous studies[6] revealed that the ground state of the Pd_3 cluster corresponds to nearly degenerate triplet $^3B_2$ and $^3B_1$ states (under C_{2v}), with the former state being less than 1 kcal/mol more stable. The lowest singlet state, $^1A_1$, was found to lie 4.8 kcal/mol higher in energy than the lowest triplet state, $^3B_2$, at the B3LYP/BSII level. In our previous paper[5] we have tested the ability of the B3LYP method to reproduce both the proper multiplicity of the ground state and the energy difference between the lowest singlet and triplet states of the Pd_n clusters for $n = 1$ and 2. B3LYP correctly predicted the Pd atom's singlet ground state. The singlet−triplet splitting, calculated at the B3LYP/BSII level, was underestimated by 1.4 and 3.1 kcal/mol relative to the CASPT2/BSII and experimental data, respectively. Likewise, for Pd_2, the triplet ground state was found at both the CASPT2 and the B3LYP levels. The energy gap between the lowest singlet and triplet states calculated at the B3LYP/BSII level was underestimated by 3.5 kcal/mol with respect to the CASPT2 results. Thus, these data lend some credit to the B3LYP predictions of the ground-state multiplicity of Pd_n clusters.

In general, hydrogen molecules can coordinate to Pd_3 clusters via several ways. Previously, it was shown that the coordination mode through the H−H bond perpendicular to the Pd−Pd edge of Pd_3 led to the dihydride complex $Pd_3(H)_2$ without a barrier on the singlet potential energy surface (PES). A small activation barrier was present on the triplet PES, equal approximately to the S−T splitting of Pd_3 (ca. 5 kcal/mol).[6] For the singlet $Pd_3(H)_2$ product complex, three distinct isomers of (**e,e**), (**e,f**), and (**f,f**) type (cf. Section II) were found. The (**e,f**) isomer appeared to be energetically the most favorable, followed by the (**e,e**) and the (**f,f**) kinds, although the three isomers were lying within 2 kcal/mol of one another. Also, the $Pd_3(H)_2$ structures could rearrange easily (at a very low energy barrier) relative to each other.

However, in our previous paper[6] we did not present results relevant to H_2 coordination directly to one of the Pd centers. As shown in Figure 1, coordination of this type results in the formation of a weakly bound $Pd_3(H_2)$ complex, **Pd3_1_a**, with the calculated adsorption enthalpies ΔH (298.15 K) of −9.8 and −11.8 kcal/mol for the triplet and singlet states, respectively (Table 1). The corresponding values of the free energy of adsorption ΔG (298.15 K) are −3.1 and −4.6 kcal/mol. The **Pd3_1_a** initial complex rearranges subsequently via **Pd3_1_b** TS into **Pd3_1_c_(e,f)** and **Pd3_1_c_(t,e)** dihydride com-

TABLE 2: Energies and Thermodynamic Values (kcal/mol) for Reactions Involving Pd_4 Clusters Calculated at the B3LYP/BSII Level

reaction species[a]	Δ*E*		*T* = 298.15 K		*T* = 70 K	
		ΔZPE	Δ*H*	Δ*G*	Δ*H*	Δ*G*
$Pd_4(^3A'') + H_2$	0.0	0.0	0.0	0.0	0.0	0.0
$Pd_4(^1A_1) + H_2$	16.8	16.8	16.8	17.5	16.8	17.0
$Pd_4(H_2)$(**Pd4_1_a**)	6.9	9.0	8.0	16.1	8.5	10.1
$Pd_4(H_2)$ (^3A) (**Pd4_1_a**)	−8.8	−7.0	−7.7	−1.1	−7.4	−6.0
1st H_2 act TS (**Pd4_1_b**)	13.3	13.8	12.2	21.1	13.3	14.9
1st H_2 act TS (^3A)(**Pd4_1_b**)	4.4	4.0	2.8	10.5	3.5	5.0
$Pd_4(H)_2$(**Pd4_1_c_(e,e)**)	−15.5	−13.5	−14.9	−6.2	−13.9	−12.3
$Pd_4(H)_2$(**Pd4_1_c_(e,e′)**)	−20.9	−19.0	−20.3	−11.3	−19.5	−17.8
$Pd_4(H)_2$(**Pd4_1_c_(f,f)**)	−19.3	−18.3	−20.0	−10.9	−18.8	−17.2
isomer TS (**Pd4_1_d1**)	−14.6	−13.2	−14.9	−5.9	−13.7	−12.1
$Pd_4(H)_2$ (^3A)(**Pd4_1_c_(t,e)**)	0.1	1.3	0.0	8.0	0.8	2.3
migrat TS (3A)(**Pd4_1_d2**)	3.8	3.9	2.6	10.1	3.5	4.8
$Pd_4(H)_2(^3A')$(**Pd4_1_c_(e,e)**)	−4.5	−4.1	−5.3	2.4	−4.5	−3.1
$Pd_4(H)_2(^3A)$(**Pd4_1_c_(e,e′)**)	−8.3	−7.6	−8.9	−1.3	−8.1	−6.7
$Pd_4(H)_2(^3A'')$(**Pd4_1_c_(e,f)**)	−5.2	−5.1	−6.4	1.3	−5.5	−4.2
$Pd_4(H)_2$ (**Pd4_1_c_(e,e′)**) [+ mH2]	0.0	0.0	0.0	0.0	0.0	0.0
$Pd_4(H)_2(H_2)$(**Pd4_2_a_(e,e′)**)	−10.8	−9.2	−9.9	−3.7	−9.6	−8.3
$Pd_4(H)_2(H_2)$(**Pd4_2_a_(f,f)**)	−10.0	−8.8	−9.9	−3.0	−9.2	−7.9
$Pd_4(H)_2(H_2)$(**Pd4_2_a′_(f,f)**)	−9.0	−8.0	−9.0	−2.7	−8.4	−7.2
$Pd_4(H)_2(H_2)$(**Pd4_2_a_(e,f)**)	−9.2	−7.6	−8.4	−2.4	−8.0	−6.8
2nd H_2 act TS (**Pd4_2_b**)	6.5	7.1	5.6	13.5	6.7	8.0
*2nd H_2 act TS (**Pd4_2_b**) reverse*[b]	*1.3*	*0.7*	*0.7*	*0.7*	*0.7*	*0.7*
$Pd_4(H)_4$(**Pd4_2_c_(t,e,e,e)**)	5.2	6.4	4.9	12.7	6.0	7.3
$Pd_4(H)_2(H_2)_2$(**Pd4_3_a_(f,f)**)	−22.2	−19.3	−21.2	−7.6	−20.1	−17.5
$Pd_4(H)_2(H_2)_2$(**Pd4_3_a_(e,e′)**)	−21.0	−17.7	−19.1	−6.2	−18.5	−15.9
$Pd_4(H)_2(H_2)_2$(**Pd4_3_a′_(f,f)**)	−20.5	−17.6	−19.4	−6.0	−18.4	−15.8
$Pd_4(H)_2(H_2)_2$(**Pd4_3_a′_(e,e′)**)	−20.4	−16.5	−18.2	−4.8	−17.3	−14.7
$Pd_4(H)_2(H_2)_3$(**Pd4_4_a_(e,e′)**)	−31.4	−25.4	−28.0	−7.8	−26.7	−22.7
$Pd_4(H)_2(H_2)_4$(**Pd4_5_a_(e,e′)**)	−43.2	−34.3	−38.0	−10.1	−36.0	−30.6

[a] If not indicated, the electronic state of the system is a closed-shell singlet. [b] Relative to the $Pd_4(H)_4$(**Pd4_2_c_(t,e,e,e)**) product.

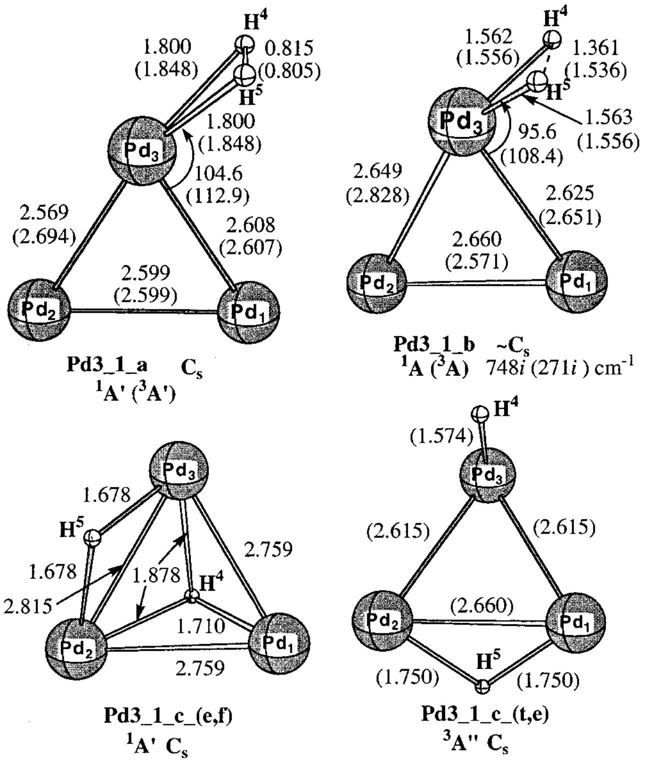

Figure 1. B3LYP/BSI optimized structures pertinent to the reaction of Pd_3 with the first H_2 (bond lengths in Å, angles in degrees); numbers in parentheses are for triplet states. Magnitudes of imaginary frequencies are included for the TSs.

plexes, respectively, on the singlet and triplet PESs (Figure 1). This finding has been confirmed by following the IRC from both transition states (note that the **Pd3_1_c_(e,f)** complex was previously reported[6] as **Pd3_H_Com1**). The H−H activation barriers $\Delta H^{\ddagger}$ (298.15 K) from **Pd3_1_a** are 3.9 and 7.2 kcal/mol on the singlet and triplet PESs, respectively. Thus, with Δ*H* (298.15 K), the singlet first H_2 activation TS lies 7.9 kcal/mol lower than the $Pd_3(^1A_1) + H_2$ singlet reactants, whereas its triplet counterpart lies 2.6 kcal/mol lower than corresponding $Pd_3(^3B_2) + H_2$ reactants. With Δ*G* (298.15 K), the singlet **Pd3_1_b** is located 0.3 kcal/mol below the $Pd_3(^1A_1) + H_2$ asymptote, whereas the triplet TS lies 3.7 kcal/mol above the $Pd_3(^3B_2) + H_2$ asymptote.

B. Reaction/Adsorption of One or More H_2 Molecules with the $Pd_3(H)_2$ Complex. Next we discuss the reaction of $Pd_3(H)_2$ with H_2 molecules. Because $Pd_3(H)_2$ has three different, but energetically very close isomers,[6] **Pd3_1_c_(e,e)**, **Pd3_1_c_(e,f)**, and **Pd3_1_c_(f,f)**, we have investigated the reaction of all these isomers with the second H_2. Various Pd_3H_4 structures were probed, and the resulting minima are shown in Figure 2. Of these, **Pd3_2_a_(e,f)**, **Pd3_2_a_(e,e)**, and **Pd3_2_a′_(e,f)** are dihydrogen complexes. According to Table 1, adsorption of H_2 onto $Pd_3(H)_2$ to give **Pd3_2_a_(e,f)**, **Pd3_2_a_(e,e)**, and **Pd3_2_a′_(e,f)** is exothermic at 298.15 K with the enthalpies of adsorption Δ*H* of −11.7, −8.6, and −10.0 kcal/mol, and free energies of adsorption Δ*G* of −5.6, −1.7, and −3.1 kcal/mol, respectively. The basis set superposition error (BSSE) calculated by the full counterpoise method[17] and BSII did not exceed 0.13 kcal/mol for the binding energy (−Δ*E*) of these complexes.

Unlike the case of $Pd_3(H)_2$, no stable $Pd_3(H)_4$ structure (with zero imaginary frequencies) that contains two dissociated H_2 molecule in "**e**" or "**f**" positions was found. We did find a **Pd3_2_c** structure of this type under a C_s symmetry constraint, but it produced one imaginary frequency; following the corresponding mode led eventually to the $Pd_3(H)_2(H_2)$ complex,

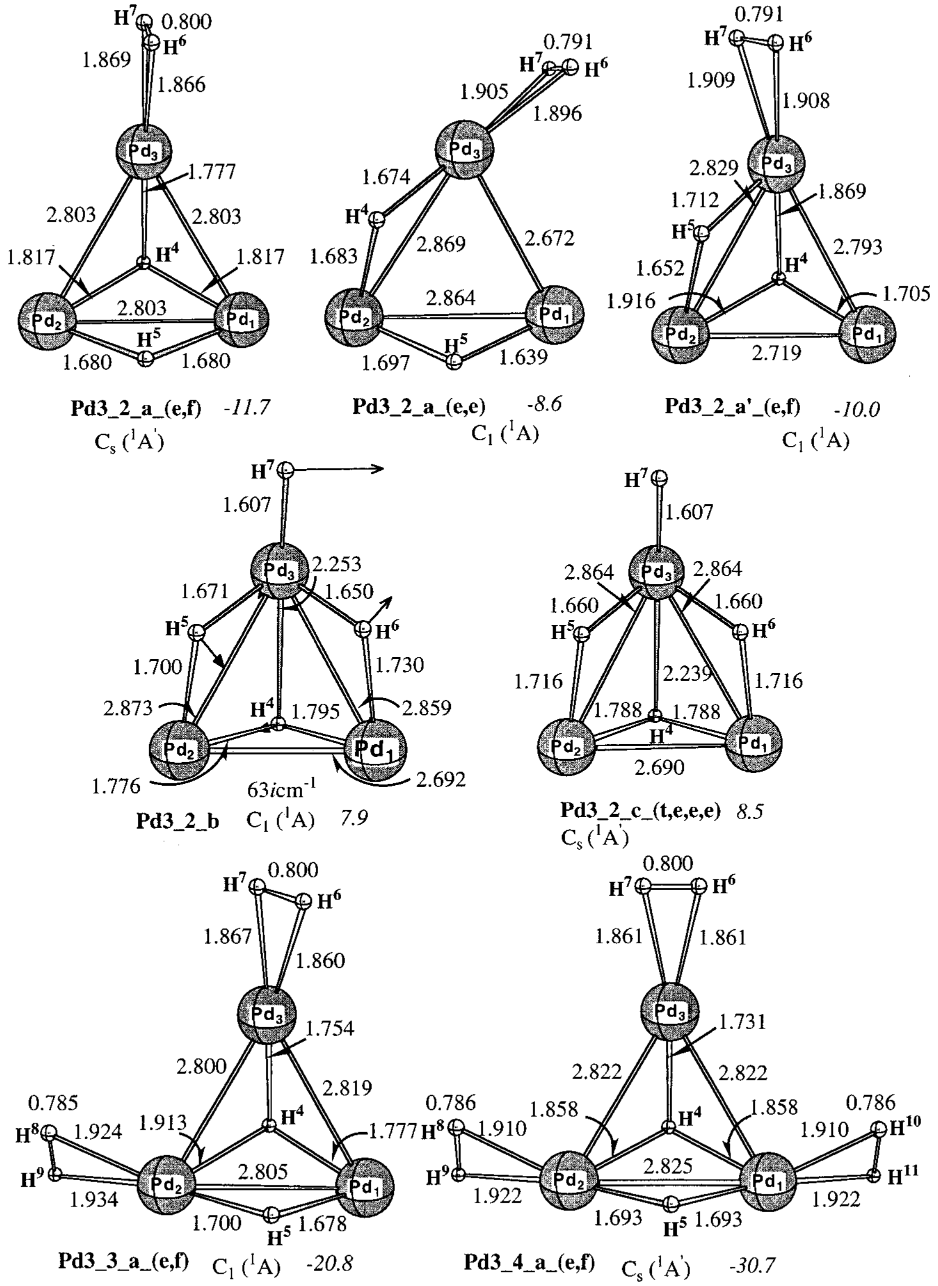

Figure 2. B3LYP/BSI optimized structures pertinent to the reactions of $Pd_3(H)_2$ with one, two, and three H_2 molecules (bond lengths in Å). Values shown in italics are ΔH (298.15 K) relative to the ground-state reactants, $Pd_3(H)_2 + mH_2$ (see Table 1). The reaction coordinate vector and the corresponding imaginary frequency are shown for the TS.

Pd3_2_a_(e,e). Instead, a $Pd_3(H)_4$ structure holding one H in a "**t**" position and corresponding to a genuine minimum, **Pd3_2_c_(t,e,e,e)**, was found (Figure 2). This $Pd_3(H)_4$ lies 8.5 (ΔH at 298.15 K) and 16.5 (ΔG at 298.15 K) kcal/mol above the reactants $Pd_3(H)_2$ (**Pd3_1_c_(e,f)**) + H_2. The computed pathway of this reaction follows a route where the second H_2 is first bound in $Pd_3(H)_2(H_2)$ (**Pd3_2_a_(e,f)**) and then activated at the productlike TS (**Pd3_2_b**) (Figure 2). Activation enthalpy $\Delta H^{\ddagger}$ (298.15 K) for the latter step is 7.9 kcal/mol with respect to $Pd_3(H)_2 + H_2$; for the reverse process (at the B3LYP/BSII//B3LYP/BSI level), this enthalpy is negative by 0.5 kcal/mol (Table 1). Therefore, $Pd_3(H)_4$ (**Pd3_2_c_(t,e,e,e)**) containing two dissociated H_2 molecules would not exist either kinetically or thermodynamically. In summary, the reaction of $Pd_3(H)_2$ with H_2 molecules gives only complex $Pd_3(H)_2(H_2)$, where the second H_2 is not activated. Thermodynamically, the most favorable structure of $Pd_3(H)_2(H_2)$ is that of **Pd3_2_a_(e,f)** with C_s symmetry.

Our calculations show that the **Pd3_2_a_(e,f)** complex can accept two additional H_2 molecules to its "naked" ("unsaturated") Pd centers (see Figure 2 and Table 1). At 298.15 K, the computed enthalpies of reaction for adsorption of $2H_2$ and $3H_2$ onto $Pd_3(H)_2$ to form $Pd_3(H)_2(H_2)_2$ (**Pd3_3_a_(e,f)**) and $Pd_3(H)_2(H_2)_3$ (**Pd3_4_a_(e,f)**) are −20.8 and −30.7 kcal/mol, respectively. The corresponding free energies of adsorption ΔG (298.15 K) are −7.2 and −10.1 kcal/mol (Table 1). The hydrogen-saturated Pd_3 cluster, $Pd_3(H)_2(H_2)_3$, holds one dissociated and three "slightly activated" H_2 molecules (the latter with the H−H bond-lengths increase of 0.04−0.06 Å and H−Pd distances of 1.86−1.92 Å) and exhibits a H/Pd ratio of 2.7. Comparison of the thermodynamics of the reactions $Pd_3(H)_2 + mH_2 \rightarrow Pd_3(H)_2(H_2)_m$ ($m = 1-3$) at $T = 298.15$ and 70 K

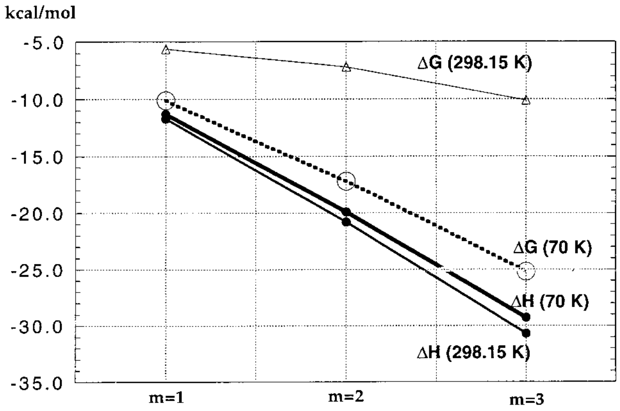

Figure 3. Profiles of ΔH (298.15 and 70 K) and ΔG (298.15 and 70 K) for the $Pd_3(H)_2 + mH_2 \rightarrow Pd_3(H)_2(H_2)_m$ ($m = 1-3$) reaction as functions of m. For $m = 1$, the values for the most stable complex, $Pd_3(H)_2(H_2)$ (**Pd3_2_a_(e,f)**), are used.

(Figure 3, Table 1) indicates the following: (1) At $T = 298.15$ K, an unfavorable entropy contribution in free energy ($-T\Delta S$) is significant and increases strongly with m; (2) At 70 K, the entropy contribution affects ΔG to a much lesser extent. (3) The heats of reaction calculated at 70 K are −11.3, −19.9, and −29.3 kcal/mol using ΔH, whereas they are −10.1, −17.2, and −25.2 kcal/mol using ΔG for $m = 1$, 2, and 3, respectively. Alternatively, the heats of reaction calculated at 70 K for the $Pd_3(H)_2(H_2)_{m-1} + H_2 \rightarrow Pd_3(H)_2(H_2)_m$ ($m = 1-3$) process, i.e., for adsorption of the consecutive H_2 molecules, are found to be −11.3, −8.6, and −9.4 kcal/mol (ΔH), and −10.1, −7.1, and −8.0 kcal/mol (ΔG) for $m = 1$, 2, and 3, respectively.

C. Bare Pd_4 Cluster. The bare Pd_4 cluster has been the subject of INDO-MRCIS,[18] ab initio (SCF- and CASSCF-based)[19,20] and a variety of DFT[20−22] studies. All these studies concluded that the ground-state of Pd_4 is a tetrahedral-like triplet state. In particular, extensive calculations at the multireference configuration interaction (CI) with single and double excitations (MRSDCI)[19] and DFT[20] levels (using relativistic ECP) consistently predicted that the linear, square, and rhomboid planar structures of Pd_4 would be significantly higher in energy compared to the tetrahedral arrangement for both triplet and singlet multiplicities. Our thorough studies of the structure and stability of the Pd_4 cluster also led to the same conclusion. Therefore, we will discuss in detail only the thermodynamically most favorable tetrahedral-like structures of Pd_4. Our data for the square and rhomboid planar structures of Pd_4 are presented in the Supporting Information.

Jahn−Teller distortion of the triplet T_d ($^3T_2$) structure of Pd_4 to C_{2v} symmetry was predicted to stabilize the cluster only slightly (1.6 kcal/mol), in accordance with the earlier result.[18] Here, we found that the distorted $C_{2v}(^3B_2)$ structure, reported[22] to be ground state at the B3LYP level, shows one imaginary frequency and distorts further to the C_s ($^3A''$) structure (see Figure 4).[23a] The triplet ground-state structure of Pd_4 has Pd−Pd distances of 2.60−2.72 Å, which can be compared with the MRSDCI bond length of 2.69 Å[19] and other DFT distances of 2.58−2.76 Å[20] and 2.60−2.78 Å.[22,23b] The lowest singlet state of Pd_4 ($^1A_1$) derives from the D_{2d} structure (Figure 4) and lies 16.8 kcal/mol above the triplet (Table 2).[24] This value of the singlet−triplet splitting, calculated at the B3LYP/BSII level, may be underestimated by ca. 5 kcal/mol, considering the results for Pd_2.[5] It is in a good agreement with the previous DFT results[20,22] of 16.1 and 16.7 kcal/mol but is substantially larger than the MRSDCI (MRSDCI + Q)[19] and INDO-MRCIS[18] values of 0.4 (1.2) and 8.8 kcal/mol, respectively.

D. Activation of the First H_2 on Pd_4. As expected, in the first step of the reaction between Pd_4 cluster and H_2 molecule, the dihydrogen complex $Pd_4(H_2)$ is formed (structure **Pd4_1_a** in Figure 4). The ground state of this complex is a triplet, with the singlet state lying 15.7 kcal/mol higher. The calculated enthalpies of the reaction $Pd_4 + H_2 \rightarrow Pd_4(H_2)$ are −7.7 and −8.8 kcal/mol for the triplet and singlet states, respectively (Table 2 and Figure 5). In the next step, the activation of H_2

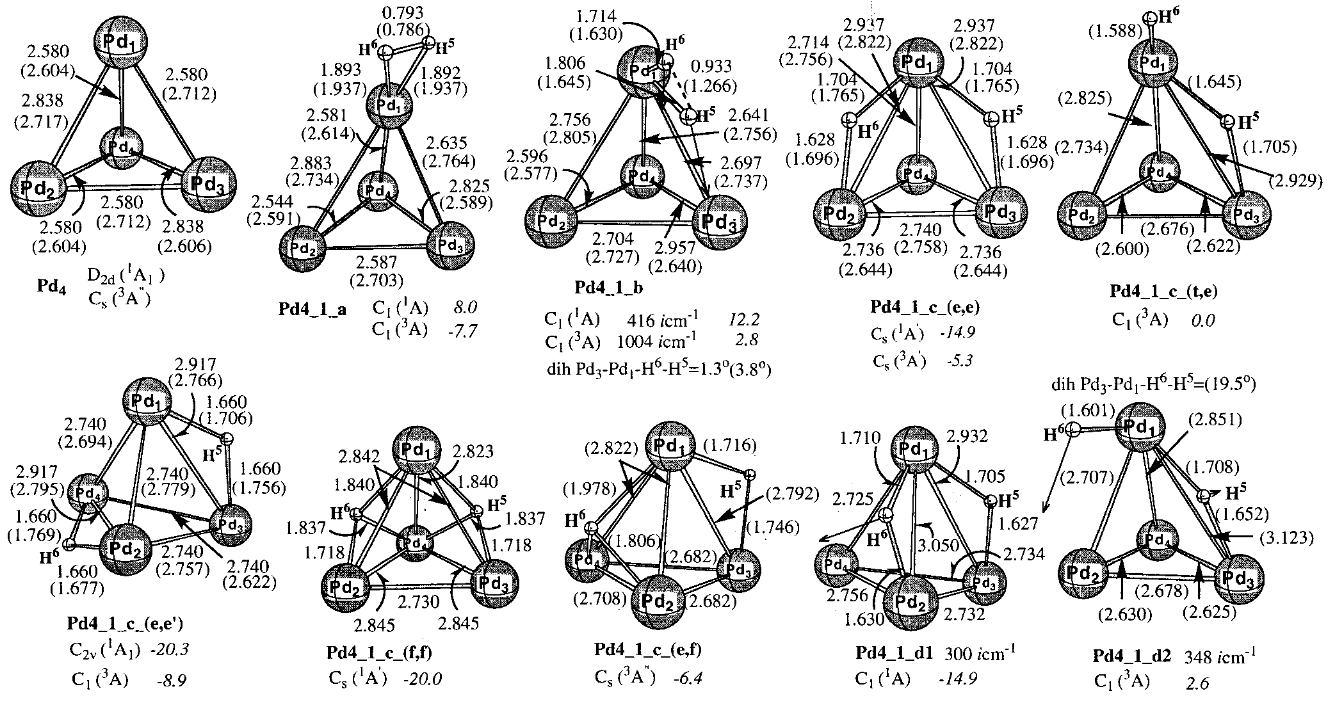

Figure 4. B3LYP/BSI optimized structures pertinent to the reactions of Pd_4 with the first H_2 (bond lengths in Å); geometrical parameters in parentheses are for triplet states. Values shown in italics are ΔH (298.15 K) relative to the ground-state reactants, Pd_4 ($^3A''$) + H_2 (see Table 2). The reaction coordinate vector and the corresponding imaginary frequency are shown for each TS.

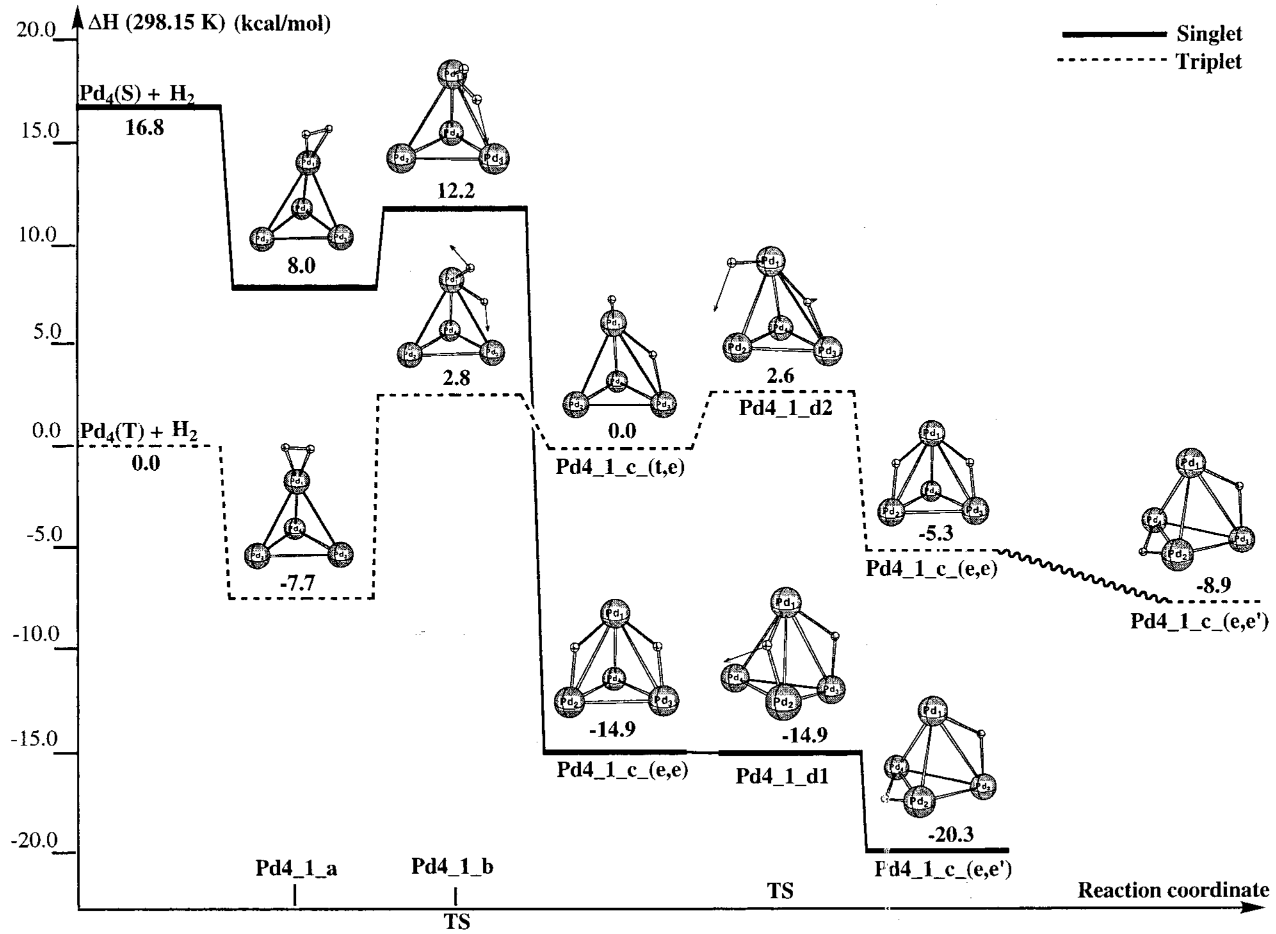

Figure 5. Profiles of ΔH (298.15 K) for activation of the first H_2 on Pd_4.

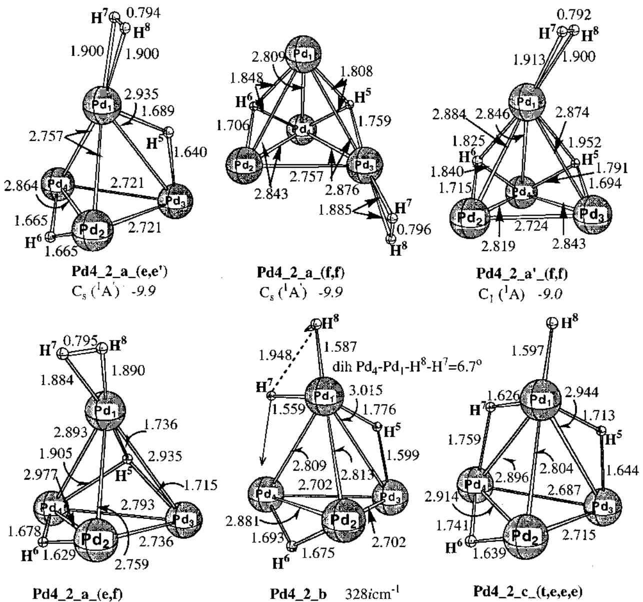

Figure 6. B3LYP/BSI optimized structures pertinent to the reactions of $Pd_4(H)_2$ with one H_2 (bond lengths in Å). Values shown in italics are ΔH (298.15 K) relative to the ground-state reactants, $Pd_4(H)_2$ + mH_2 (see Table 2). The reaction coordinate vector and the corresponding imaginary frequency are shown for the TS.

takes place via transition state **Pd4_1_b**, which involves breaking an H−H bond and forming the $Pd_4(H)_2$ complex. Interestingly, on the singlet PES the first H_2 activation TS lies 4.6 kcal/mol below the $Pd_4(S) + H_2$ asymptote, whereas on the triplet PES this TS is 2.8 kcal/mol higher than the corresponding $Pd_4(T) + H_2$ asymptote (Figure 5).

In terms of H−H bond length, the singlet TS **Pd4_1_b** is an "early" saddle point (r(H−H) = 0.93 Å), with the H−H bond being broken positioned "parallel" to one of the Pd−Pd edges. Following the IRC from **Pd4_1_b** on the singlet PES, this TS was found to connect the initial complex **Pd4_1_a** with the **Pd4_1_c_(e,e)** product, wherein the two H-ligands bridge the edges sharing the Pd atom (Figure 4). Complex **Pd4_1_c_(e,e)** is predicted to be 23 kcal/mol more stable than the initial complex **Pd4_1_a**, but it is not the thermodynamically most favorable isomer of $Pd_4(H)_2$. Indeed, our calculations reveal that the structure **Pd4_1_c_(e,e)**, of C_s symmetry, easily isomerizes to a more stable structure **Pd4_1_c_(e,e′)**, of C_{2v} symmetry, another "edge−edge" type isomer, where the two H-ligands bridge the Pd−Pd edges not sharing the Pd atom. **Pd4_1_c_(e,e′)** is 5.4 kcal/mol more stable than **Pd4_1_c_(e,e)** and lies 20.3 kcal/mol below the ground-state reactants $Pd_4(T) + H_2$. This isomerization process occurs through transition state **Pd4_1_d1** and involves movement of H from one edge site to the another via the adjacent face site (see Figure 4). The Pd−H distances in **Pd4_1_c_(e,e)** and **Pd4_1_c_(e,e′)** of 1.63−1.70 Å can be compared with the experimentally observed Pd−H bond lengths in $(\Delta\text{-H})_2Pd_2$ compounds (1.62−1.79 Å).[26] Another singlet $Pd_4(H)_2$ isomer we found, **Pd4_1_c_(f,f)**, features both H atoms occupying the face sites and is only 0.3 kcal/mol less stable than **Pd4_1_c_(e,e′)** (Table 2). The **Pd4_1_c_(e,e′)** → **Pd4_1_c_(f,f)** isomerization is likewise anticipated to be a low-barrier reaction and was not pursued here.

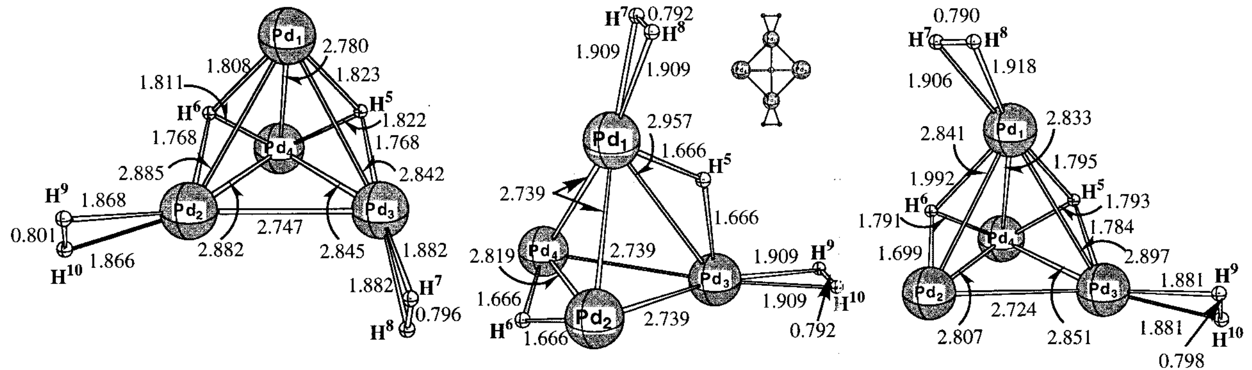

Pd4_3_a_(f,f)
C_1 (^1A) $Pd_4(H)_2(H_2)_2$ *-21.2*

Pd4_3_a_(e,e')
C_{2v} ($^1A_1$) $Pd_4(H)_2(H_2)_2$ *-19.1*

Pd4_3_a'_(f,f)
C_1 (^1A) $Pd_4(H)_2(H_2)_2$ *-19.4*

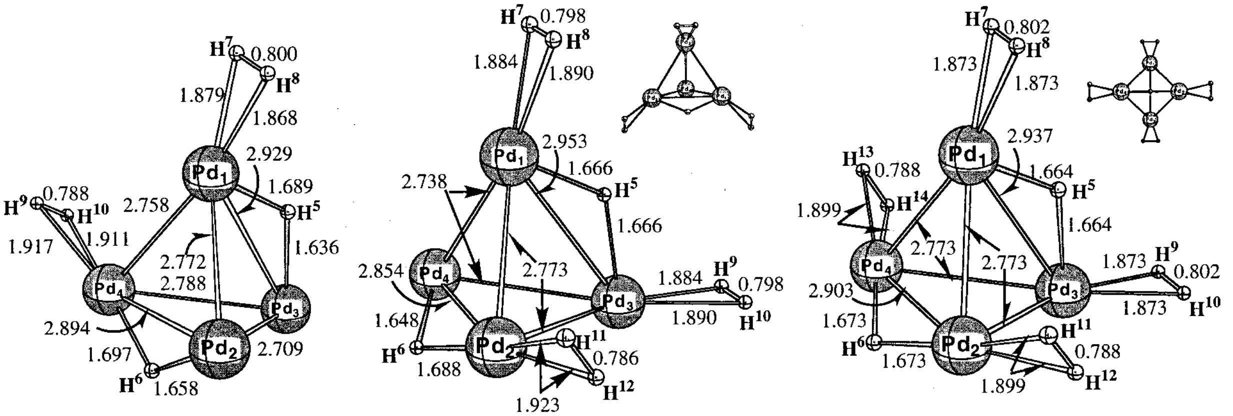

Pd4_3_a'_(e,e')
C_1 (^1A) $Pd_4(H)_2(H_2)_2$ *-18.2*

Pd4_4_a_(e,e')
C_s ($^1A'$) $Pd_4(H)_2(H_2)_3$ *-28.0*

Pd4_5_a_(e,e')
C_{2v} ($^1A_1$) $Pd_4(H)_2(H_2)_4$ *-38.0*

Figure 7. B3LYP/BSI optimized structures pertinent to the reactions of $Pd_4(H)_2$ with two, three, and four H_2 molecules (bond lengths in Å). Values shown in italics are ΔH (298.15 K) relative to the ground-state reactants, $Pd_4(H)_2 + mH_2$ (see Table 2).

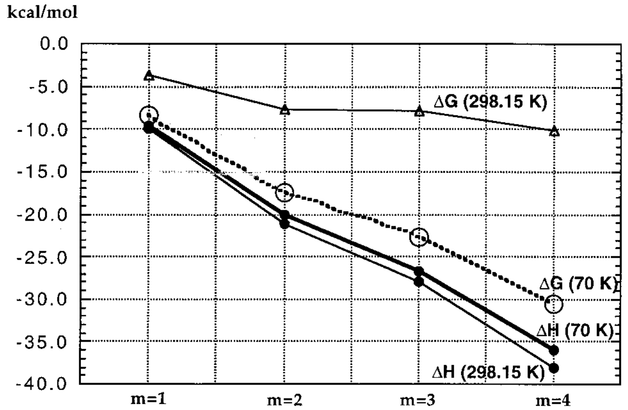

Figure 8. Profiles of ΔH (298.15 and 70 K) and ΔG (298.15 and 70 K) for the $Pd_4(H)_2 + mH_2 \rightarrow Pd_4(H)_2(H_2)_m$ ($m = 1-4$) reaction as functions of m. For $m = 1$ and 2, the values for the most stable complexes, $Pd_4(H)_2(H_2)$ (**Pd4_2_a_(e,e′)** and $Pd_4(H)_2(H_2)_2$ (**Pd4_3_a_(f,f)**), respectively, are used.

On the triplet PES, activation of the first H_2 proceeds through a similar TS, **Pd4_1_b**, while a barrier height calculated from the initial complex **Pd4_1_a** is 10.5 kcal/mol (on the singlet PES it is only 4.2 kcal/mol; see Figure 5). The net activation enthalpy at 298.15 K relative to the Pd_4(T) + H_2 asymptote is found to be 2.8 kcal/mol, as mentioned above. The triplet TS **Pd4_1_b** appears later along the reaction coordinate (r(H−H) =1.27 Å) as compared to its singlet counterpart, but again the H−H activation takes place in "parallel" to the Pd−Pd edge (Figure 4). Following the IRC from **Pd4_1_b** on the triplet PES, one finds that this transition state connects the initial complex **Pd4_1_a** with the product **Pd4_1_c_(t,e)**, in which one H is bound to the single Pd atom, and the second H bridges the Pd−Pd edge (note that no singlet analogue of this structure was found). **Pd4_1_c_(t,e)** rearranges rather easily via migration of the TS, **Pd4_1_d2**, to the more stable isomer **Pd4_1_c_(e,e)**. The latter isomer rearranges further to the most stable triplet $Pd_4(H)_2$ structure, **Pd4_1_c_(e,e′)**, wherein both hydrogens occupy the edge sites not sharing the Pd atom. Recall that this kind of structure is most favorable in the singlet state as well. Because we have shown that **(e,e)** → **(e,e′)**-type isomerization occurs on the singlet PES with a very low energetic barrier, we did not study the triplet case in more detail. The triplet structures **Pd4_1_c_(e,e)** and **Pd4_1_c_(e,e′)** are ca. 10 kcal/mol less stable in ΔH (298.15 K) than their singlet counterparts and show correspondingly longer Pd−H bonds, by 0.02−0.11 Å. The second stable triplet $Pd_4(H)_2$ isomer, **Pd4_1_c_(e,f)**, shows a unique "edge-face" structure, not existing for the singlet state (Figure 4),[27] and lies only 2.5 kcal/mol higher than **Pd4_1_c_(e,e′).**

Past the first H_2 activation TS, the singlet PES goes down below the triplet one, and as a consequence, it crosses the triplet PES in this region (see Figure 5). Assuming the $Pd_4 + H_2$ reaction starts on the ground-state triplet PES, this behavior implies that (1) the triplet **Pd4_1_b** determines the actual first H_2 activation barrier, and (2) the reaction will subsequently proceed on the singlet PES if the coupling element between the singlet and the triplet is sufficiently large (Pd is heavy enough that spin−orbit effects on this reaction can be expected to be important).

In this regard we notice the recent paper by Moc et al.,[25b] in which the B3LYP spin–crossover points found along the reaction coordinate were consistent with those predicted at the higher multiconfigurational second-order quasidegenerate perturbation theory (MCQDPT2) level.

E. Reaction/Adsorption of One or More H_2 Molecules with a $Pd_4(H)_2$ Complex. A large number of Pd_4H_4 structures were examined, and the most stable ones are summarized in Figure 6. An open $Pd_4(H)_4$ cluster, **Pd4_2_c_(t,e,e,e)**, comprises two dissociated H_2 molecules,[28] whereas $Pd_4(H)_2(H_2)$ species **Pd4_2_a_(e,e′)**, **Pd4_2_a_(f,f)**, **Pd4_2_a′_(f,f)** and **Pd4_2_a_(e,f)** include both dissociated and molecular H_2. Adsorption of H_2 onto $Pd_4(H)_2$ to form $Pd_4(H)_2(H_2)$ is predicted to be exothermic, where the computed ΔH (298.15 K) values fall in the range between −8.4 and −9.9 kcal/mol. Similarly, the ΔG (298.15 K) is calculated to range between −2.4 and −3.7 kcal/mol for those reactions (Table 2). Among the four $Pd_4(H)_2(H_2)$ isomers found, **Pd4_2_a_(e,e′)** and **Pd4_2_a_(f,f)** are the most stable.

In contrast, dissociative adsorption, $Pd_4(H)_2 + H_2 \rightarrow Pd_4(H)_4$(**Pd4_2_c_(t,e,e,e)**), is predicted to be endothermic (the calculated ΔH is 4.9 kcal/mol at 298.15 K) and proceeds with a 5.6 kcal/mol barrier ($\Delta H^{\ddagger}$ (298.15 K) relative to $Pd_4(H)_2 + H_2$ at the productlike TS **Pd4_2_b** (Figure 6). As the energetic barrier for the reverse reaction is only 0.7 kcal/mol (Table 2), the $Pd_4(H)_4$ cluster **Pd4_2_c_(t,e,e,e)** is kinetically and thermodynamically unstable.

Thus, the results presented in this section demonstrate that the complex $Pd_4(H)_2$ does not activate the second H_2 molecule. Instead, it forms a molecular complex, $Pd_4(H)_2(H_2)$, whose most favorable structures are **Pd4_2_a_(e,e′)** and **Pd4_2_a_(f,f)**, with the second H_2 coordinated to one of the Pd centers and three other Pd centers left “naked”. One may therefore expect that these “naked” Pd centers are able to bind additional H_2 molecules as in the Pd_3 case. Indeed, our calculations show that $Pd_4(H)_2$ takes up totally four additional H_2 molecules. The structures illustrating the binding of two, three, and four H_2 molecules are depicted in Figure 7. The ΔH and ΔG (at 298.15 K) values for adsorption of $2H_2$ onto $Pd_4(H)_2$ to form $Pd_4(H)_2(H_2)_2$ range from −18.2 to −21.2 kcal/mol and from −4.8 to −7.6 kcal/mol, respectively (Table 2). Likewise, the calculated heats of the $Pd_4(H)_2 + 3H_2 \rightarrow Pd_4(H)_2(H_2)_3$ and $Pd_4(H)_2 + 4H_2 \rightarrow Pd_4(H)_2(H_2)_4$ reactions is −28.0 and −38.0 kcal/mol using ΔH (298.15 K) and −7.8 and −10.1 kcal/mol using ΔG (298.15 K), respectively (Table 2). The hydrogen-saturated Pd_4 cluster **Pd4_5_a_(e,e′)**, of C_{2v} symmetry, holds one dissociatively and four molecularly adsorbed H_2 molecules and exhibits a H/Pd ratio of 2.5. The thermodynamic values for the reactions $Pd_4(H)_2 + mH_2 \rightarrow Pd_4(H)_2(H_2)_m$ ($m = 1-4$) at 298.15 and 70 K are compared in Figure 8. The main findings from Figure 8 parallel those for Pd_3 case (Figure 3). Also, similar to the Pd_3 case, the estimated heats of reaction at 70 K of the $Pd_4(H)_2(H_2)_{m-1} + H_2 \rightarrow Pd_4(H)_2(H_2)_m$ ($m = 1-4$) process, i.e., for adsorption of the consecutive H_2 molecules, are −9.6, −10.5, −6.6, and −9.3 kcal/mol (using ΔH values) and −8.3, −9.2, −5.2, and −7.9 kcal/mol (using ΔG values) for $m = 1$, 2, 3, and 4, respectively.

IV. Conclusions

In the present work, reaction and adsorption of multiple H_2 molecules on Pd_3 and Pd_4 clusters were investigated at the B3LYP level. From a thorough study of the PESs involved and detailed thermodynamic considerations, we have established the following:

(1) The reaction of Pd_3 (triplet ground state) with an H_2 molecule is initiated by the formation of the $Pd_3(H_2)$ dihydrogen complex. Negative net activation enthalpy is found for the overall Pd_3(triplet) + $H_2 \rightarrow Pd_3(H)_2$ (singlet) process.

(2) The reaction of Pd_4 (triplet ground state) with an H_2 molecule is initiated by the formation of the $Pd_4(H_2)$ dihydrogen complex. Because of the larger thermodynamic stability of the singlet dihydride complex $Pd_4(H)_2$ (dissociative adsorption product) relative to the triplet counterpart, a spin–crossing should occur to move the reaction to the singlet PES.

(3) The overall Pd_4(triplet) + $H_2 \rightarrow Pd_4(H)_2$ (singlet) reaction is calculated to be exothermic, ΔH (298.15 K) = −20.3 kcal/mol, with a net activation enthalpy at 298.15 K of 3 kcal/mol.

(4) Among various possible isomers of the singlet $Pd_4(H)_2$, the most stable is **Pd4_1_c_(e,e′)**, where the two hydride ligands bridge the edges of the Pd–Pd bonds not sharing the same Pd atom. The second stable possible isomer is **Pd4_1_c_(f,f)**, in which the hydride ligands cap the faces of the Pd–Pd–Pd planes.

(5) Dissociative adsorption of the second H_2 via the $Pd_3(H)_2 + H_2 \rightarrow Pd_3(H)_4$ and $Pd_4(H)_2 + H_2 \rightarrow Pd_4(H)_4$ reactions is not feasible, as the products lack both thermodynamic and kinetic stability.

(6) Consistent with the experimental $Pd_n + D_2$ saturation studies by Cox et al.,[4] $Pd_3(H)_2$ and $Pd_4(H)_2$ complexes are found to adsorb additional mH_2 molecules. The resultant $Pd_3(H)_2(H_2)_m$ ($m = 1-3$) and $Pd_4(H)_2(H_2)_m$ ($m = 1-4$) species are stable at low temperatures (because of decreased unfavorable entropy contribution), as indicated by the computed ΔG (70 K) values for the relevant reactions. Our hydrogen-saturated clusters, $Pd_3(H)_2(H_2)_3$ and $Pd_4(H)_2(H_2)_4$, exhibit H/Pd ratios of 2.7 and 2.5, respectively.[29]

Acknowledgment. J.M. acknowledges the Emerson Center for the Visiting Fellowship. He also thanks the staff of the Emerson Center for kind help and for the use of the computer facilities and programs. The authors thank Dr. Q. Cui for his help at the early stage of this project. The present research is in part supported by a grant (CHE-9627775) from the National Science Foundation. Acknowledgment is also made for generous support of computing time at the Emerson Center of Emory University and the U.S. National Center for Supercomputing Applications (NCSA).

Supporting Information Available: Tables giving Cartesian coordinates of all the structures discussed in the paper, tables including energies and thermodynamic values for reactions involving Pd_3 and Pd_4 clusters as calculated at the B3LYP/BSI level, and a figure of bare Pd_4 cluster planar isomer structures. This information is available free of charge via the Internet at http://pubs.acs.org.

References and Notes

(1) See, for example: (a) *Physics and Chemistry of Finite Systems: From Clusters to Crystals*; Jena, P., Khanna, S. N., Rao, B. K., Eds.; Kluwer Academic: Dordrecht, 1992. (b) *Chemical Reactions in Clusters*; Berstein, E. R., Ed.; Oxford University Press: New York, 1996. (c) *Clusters of Atoms and Molecules: Theory, Experiment, and Clusters of Atoms*; Haberland, H., Ed.; Springer-Verlag: New York, 1994.

(2) See, for example: Knickelbein, M. B.; Koretsky, G. M.; Jackson, K. A.; Pederson, M. R.; Hajnal, Z. *J. Chem. Phys.* **1998**, *109*, 10692 and references therein.

(3) See, for example: (a) Whetten, R. L.; Cox, D. M.; Trevor, D. J.; Kaldor, A. *Phys. Rev. Lett.* **1985**, *54*, 1494. (b) Guesic, M. E.; Morse, M. D.; Smalley, R. E. *J. Chem. Phys.* **1985**, *82*, 590. (c) Zakin, M. R.; Cox, D. M.; Kaldor, A. *J. Chem. Phys.* **1987**, *87*, 5046. (d) Nakajima, A.; Kishi, T.; Sone, Y.; Nonose, S.; Kaya, K. *Z. Phys. D* **1991**, *19*, 385. (e) Kaldor, A.; Cox, D. M.; Zakin, M. R. *Adv. Chem. Phys.* **1988**, *70*, 211. (f) Trevor, D. J.; Cox, D. M.; Kaldor, A. *J. Am. Chem. Soc.* **1990**, *112*, 3742. (g) Geusic, M. E.; Morse, M. D.; O’Brien, S. C.; Smalley, R. E. *Rev. Sci. Instrum.*

1985, *56*, 2123. (h) Parks, E. K.; Liu, K.; Richtsmeier, S. C.; Pobo, L. G.; Riley, S. J. *J. Chem. Phys.* **1985**, *82*, 5470. (i) Kaldor, A.; Cox, D. M. *J. Chem. Soc., Faraday Trans.* **1990**, *86*, 2459.

(4) Fayet, P.; Kaldor, A.; Cox, D. M. *J. Chem. Phys.* **1990**, *92*, 254.

(5) Cui, Q.; Musaev, D. G.; Morokuma, K. *J. Chem. Phys.* **1998**, *108*, 8418.

(6) Cui, Q.; Musaev, D. G.; Morokuma, K. *J. Phys. Chem. A* **1998**, *102*, 6373.

(7) (a) Becke, A. D. *Phys. Rev. A* **1988**, *38*, 3098. (b) Lee, C.; Yang, W.; Parr, R. G. *Phys. Rev. B* **1988**, *37*, 785. (c) Becke, A. D. *J. Chem. Phys.* **1993**, *98*, 5648.

(8) DFT has proven to yield reliable results for both properties of TM systems; see for example: (a) Bauschlicher, C. W.; Langhoff, S. R.; Partridge, H. In *Modern Electronic Structure Theory*; Yarkony, D. R., Ed.; World Scientific: London, 1995. (b) Siegbahn, P. E. M. *Adv. Chem. Phys.* **1997**, *93*, 333. (c) Ziegler, T. *Chem. Rev.* **1991**, *91*, 651. (d) Salahub, D. R.; Castro, M.; Fourinier, R.; Calaminici, P.; Godbout, N.; Goursot, A.; Jamorski, C.; Kobayashi, J.; Martinez, A.; Papai, I.; Proyonov, E.; Russo, N.; Sirois, S.; Ushio, J.; Vela, A. In *Theoretical and Computational Approaches to Interface Phenomena*; Sellers, H., Olab, J., Eds.; Plenum Press: New York, 1995; p 187. (e) Musaev, D. G.; Morokuma, K. *J. Phys. Chem.* **1996**, *100*, 6509.

(9) Hay, P. J.; Wadt, W. R. *J. Chem. Phys.* **1985**, *82*, 299.

(10) Dunning, T. H., Jr. *J. Chem. Phys.* **1970**, *53*, 2823.

(11) Andrae, D.; Haussermann, U.; Dolg, M.; Stoll, H.; Preuss, H. *Theor. Chim. Acta* **1990**, *77*, 123.

(12) Dunning, T. H., Jr.*J. Chem. Phys.* **1989**, *90*, 1007. Note that here, *d* functions on H were excluded from the correlation-consistent basis set.

(13) Note that BSI and BSII correspond to BSI and BSIII, respectively, in ref 6.

(14) (a) Gonzalez, C.; Schlegel, H. B. *J. Chem. Phys.* **1989**, *90*, 2154. (b) Gonzalez, C.; Schlegel, H. B. *J. Phys. Chem.* **1990**, *94*, 5523.

(15) The choice of low temperature (70 K) was based on the recent experimental infrared study[2] on the reaction of iron clusters Fe_n with H_2. The resulting $Fe_nH_p(H_2)_q$ products were examined at flow-tube temperatures in the range between 290 and 70 K.[2]

(16) Frisch, M. J.; Trucks, G. W.; Schlegel, H. B.; Scuseria, G. E.; Robb, M. A.; Cheeseman, J. R.; Zakrzewski, V. G.; Montgomery, J. A.; Stratmann, R. E.; Burant, J. C.; Dapprich, S.; Millam, J. M.; Daniels, A. D.; Kudin, K. N.; Strain, M. C.; Farkas, O.; Tomasi, J.; Barone, V.; Cossi, M.; Cammi, R.; Mennucci, B.; Pomelli, C.; Adamo, C.; Clifford, S.; Ochterski, J.; Petersson, G. A.; Ayala, P. Y.; Cui, Q.; Morokuma, K.; Malick, D. K.; Rabuck, A. D.; Raghavachari, K.; Foresman, J. B.; Cioslowski, J.; Ortiz, J. V.; Stefanov, B. B.; Liu, G.; Liashenko, A.; Piskorz, P.; Komaromi, I.; Gomperts, R.; Martin, R. L.; Fox, D. J.; Keith, T.; Al-Laham, M. A.; Peng, C. Y.; Nanayakkara, A.; Gonzalez, C.; Challacombe, M.; Gill, P. M. W.; Johnson, B.; Chen, W.; Wong, M. W.; Andres, J. L.; Head-Gordon, M.; Replogle, E. S.; Pople, J. A. *Gaussian 98*, Revision A.1; Gaussian, Inc.: Pittsburgh, PA, 1998.

(17) Boys, S.; Bernardi, F. *Mol. Phys.* **1970**, *19*, 553.

(18) Estiu, G. L.; Zerner, M. C. *J. Phys. Chem.* **1994**, *98*, 4793.

(19) Dai, D.; Balasubramanian, K. *J. Chem. Phys.* **1995**, *103*, 648. Jahn−Teller distortion of the triplet $Pd_4(T_d)$ structure was not considered by these authors.

(20) Zacarias, A. G.; Castro, M.; Tour, J. M.; Seminario, J. M. *J. Phys. Chem. A* **1999**, *103*, 7692.

(21) Goursot, A.; Papai, I.; Salahub, D. R. *J. Am. Chem. Soc.* **1992**, *114*, 7452.

(22) Valerio, G.; Toulhout, H. *J. Phys. Chem.* **1996**, *100*, 10827.

(23) (a) The $C_s(^3A')$ structure of Pd_4 was ca. 0.3 kcal/mol less stable than the C_s ($^3A''$) one and had an imaginary frequency. (b) The atomization energy of Pd_4, 109.9 kcal/mol ($\Delta E+\Delta ZPE$), agrees reasonably well with the MRSDCI and other DFT values of 117 kcal/mol[19] and 114.9 and 118.2 kcal/mol,[20,22] respectively.

(24) The D_{2d} point group for the lowest singlet Pd_4 structure also emerged from another DFT study,[25] whereas only the S_4 subgroup was reported to be the singlet Pd_4 lowest-energy structure in ref 22; our Pd−Pd distances for the singlet Pd_4 remain in close agreement with those computed in refs 22 and 25.

(25) (a) Harada, M.; Dexpert, H. *J. Phys. Chem.* **1996**, *100*, 565. Only the singlet state of Pd_4 was considered by these authors. (b) Moc, J.; Fedorov, D. G.; Gordon, M. S. *J. Chem. Phys*. **2000**, 112, 10247

(26) (a) Fryzuk, M. D.; Lloyd, B. R.; Clentsmith, G. K. B.; Rettig, S. J. *J. Am. Chem. Soc.* **1991**, *113*, 4332. (b) Fryzuk, M. D.; Lloyd, B. R.; Clentsmith, G. K. B.; Rettig, S. J. *J. Am. Chem. Soc.* **1994**, *116*, 3804.

(27) The C_s-symmetry-constraint calculations of the structure **Pd4_1_c_(f,f)** in the triplet state showed two imaginary frequencies.

(28) We have found several additional open-type $Pd_4(H)_4$ clusters of very similar energy to **Pd4_2_c_(t,e,e,e)**, which are not reported to save space.

(29) With reference to the Pd_4 tetramer, the conclusion of Cox et al.[4] was that the deuterium-saturated cluster exhibited D/Pd = 3, meaning at least one more D_2 adsorbed on Pd_4 as compared to our hydrogen-saturated cluster (**Pd4_5_a_(e,e′)**).